Hardware Phenomenological Effects on Cochannel Full-Duplex MIMO Relay Performance

D. W. Bliss, *IEEE Senior Member*, T. M. Hancock, *IEEE Senior Member*,
P. Schniter, *IEEE Senior Member*

Abstract— In this paper, the performance of cochannel full-duplex multiple-input multiple-output (MIMO) nodes is considered in the context of models for realistic hardware characteristics. Here, cochannel full-duplex relay indicates a node that transmits and receives simultaneously in the same frequency band. It is assumed that transmit and receive phase centers are physically distinct, enabling adaptive spatial transmit and receive processing to mitigate self-interference. The use of MIMO indicates a self-interference channel with spatially diverse inputs and outputs, although multiple modes are not employed in this paper. Rather, we focus on rank-1 transmit covariance matrices. In practice, the limiting issue for cochannel full-duplex nodes is the ability to mitigate self-interference. While theoretically a system with infinite dynamic range and exact channel estimation can mitigate the self-interference perfectly, in practice, transmitter and receiver dynamic range, nonlinearities, and noise, as well as channel dynamics, limit the practical performance. In this paper, we investigate self-interference mitigation limitations in the context of eigenvalue spread of spatial transmit and receive covariance matrices caused by realistic hardware models.

I. INTRODUCTION

When wireless networks are operating in resource-constrained environments, full-duplex relays may be a useful approach to improve communications performance. This improvement in performance can be measured by a variety of metrics, such as increasing network data throughput and reducing latency. These potential benefits come at the expense of increased system complexity and cost, and these costs may not be warranted in all situations; however, the potential improvement justifies further investigation.

Because the cochannel full-duplex relay is typically exposed to significant self-interference, all self-interference mitigation approaches are worth exploring. In this paper, we consider spatial approaches exclusively. In spatial approaches, the degrees of freedom of the relay's transmit antenna array are used to reduce the energy sent to the relay's receive array. The receive array then mitigates any self-interference residuals. In Reference [1], a combination of temporal and transmit spatial processing techniques was shown experimentally to reduce self-interference of a full-duplex multiple-input multiple-output (MIMO) relays at all of the multiple receive antennas by up to 60 dB, with additional suppression produced by

spatial isolation; however, the effectiveness of self-interference mitigation techniques was not simply multiplicative.

The focus in this paper is the development of simple hardware models for use with MIMO cochannel full-duplex relays that employ independent transmit and receive antenna arrays. Here, we use MIMO to indicate that the relay node has a channel with multiple transmit and receive antennas, although, in this paper, the multiple antennas are not used to transmit multiple streams of data.

A. Background

The advantages to networks employing nodes that can take advantage of full-duplex communications have been considered in a variety of contexts [2], [3], [4], [5], [6], including discussion of alternative performance constraints such as finite queue lengths [7]. The performance of full-duplex MIMO relays is considered in References [8], [9], [10], [11], [12], [13], including optimizing performance for a mix of half- and full-duplex operation [14], [15]. Approaches for full-duplex MIMO repeaters are discussed in Reference [16]. Full-duplex MIMO relay signal processing concepts are presented in References [8], [1], [17], [18], [19], [20], [21], [22], [20], [23], [24]. The theoretical aspects of hardware limitations of full-duplex MIMO communications are discussed in References [18], [19], [20], [25], [26], [15]. Spatial isolation of full-duplex MIMO relays is considered in References [27], [28], [29].

B. Contributions

The main contributions of the paper are that 1) we present a transmit and receive spatial processing chain; 2) we investigate the hardware issues that limit the mitigation of self-interference; 3) we present results for combined effects under reasonable hardware parameters. In so doing, we demonstrate the viability of spatial mitigation for relay self-interference mitigation; and 4) we consider transmit and receive eigenvalue spread as a method to provide intuition with respect to performance implications. The resulting receiver eigenvalue distribution affects directly the SNR at the output of the receiver, although the exact SNR depends upon the receiver implementation. We consider a somewhat simplified model of what is a very complicated system. The hardware limitations that we consider include transmit quantization, transmit noise, transmit nonlinearities, transmit in-phase and quadrature (IQ) mismatch, receive quantization, receive noise, receive nonlinearities, and receive IQ mismatch. Often analysis of full-duplex relays falls into amplify-and-forward and decode-and-forward approaches. The analysis developed in this paper can

apply to either approach, although because we discuss the effects of digital-to-analog and analog-to-digital converters, decode-and-forward relays are a more natural application.

C. Analysis Caveats

To help clarify the presentation of this analysis, we make a few simplifying assumptions. We assume that the relay has $n_{\mathcal{R},t}$ transmit antennas and $n_{\mathcal{R},r}$ receive antennas. In our simulated examples, we consider the special case in which $n_{\mathcal{R},r} = n_{\mathcal{R},t} - 1$, so that there is one more transmit antenna than receive antennas. While temporal processing is a powerful mitigation tool, in this paper, we will focus on transmit and receive spatial mitigation approaches. To aid interpretation, we employ an intended transmit covariance that is rank-1. It is assumed here that the channel is known exactly. This assumption does deserve further investigation, particularly in dynamic environments, but this topic is outside the scope of this paper. In addition, it is assumed that the channels are not frequency selective, although extensions for frequency-selective channels to the discussion presented here are possible. Finally, a relatively large number of antennas are employed in the examples ($n_{\mathcal{R},t} = 9$ and $n_{\mathcal{R},r} = 8$). In most practical systems, a smaller number of antennas will be employed. By employing a larger number of antennas, the limiting shape of the eigenvalue distribution of the transmit and receive covariance matrices is displayed.

II. SPATIAL SELF-INTERFERENCE MITIGATION

A. Ideal Relay Model

In general, networks can have an arbitrary number of sources, relays, and destinations. For study, it is often useful to consider the simplest version of this system, in which there are three nodes: source $\mathcal{S}$, relay $\mathcal{R}$, and destination $\mathcal{D}$, although large networks may have many sources and destinations simultaneously. For a given node, it is assumed that it has $n_{\{\cdot\},t}$ transmit antennas and $n_{\{\cdot\},r}$ distinct receive antennas. In general, there are four channel matrices to consider: source-to-destination $\mathbf{H}_{\mathcal{S},\mathcal{D}} \in \mathbb{C}^{n_{\mathcal{D},r} \times n_{\mathcal{S},t}}$, source to relay $\mathbf{H}_{\mathcal{S},\mathcal{R}} \in \mathbb{C}^{n_{\mathcal{R},r} \times n_{\mathcal{S},t}}$, relay to relay $\mathbf{H}_{\mathcal{R},\mathcal{R}} \in \mathbb{C}^{n_{\mathcal{R},r} \times n_{\mathcal{R},t}}$, and relay to destination $\mathbf{H}_{\mathcal{R},\mathcal{D}} \in \mathbb{C}^{n_{\mathcal{D},r} \times n_{\mathcal{R},t}}$. However, in this paper we assume that the direct source to destination channel is weak $\mathbf{H}_{\mathcal{S},\mathcal{D}} \approx \mathbf{0}$.

Suppressing explicit temporal notational dependence and a complex baseband representation, the received signal $\mathbf{z}_{\mathcal{R}} \in \mathbb{C}^{n_{\mathcal{R},r} \times 1}$ at the relay for the ideal hardware model is given by

$$\mathbf{z}_{\mathcal{R}} = \mathbf{H}_{\mathcal{R},\mathcal{R}} \mathbf{V}_{\mathcal{R}} \mathbf{s}_{\mathcal{R}} + \mathbf{H}_{\mathcal{S},\mathcal{R}} \mathbf{V}_{\mathcal{S}} \mathbf{s}_{\mathcal{S}} + \mathbf{n}_{\mathcal{R}} , \qquad (1)$$

where $\mathbf{n}_{\mathcal{R}}$ indicates the receive noise, and a set of transmit beamformers are represented by the columns of $\mathbf{V}_{\mathcal{S}} \in \mathbb{C}^{n_{\mathcal{S},t} \times n_{\mathcal{S},b}}$ and $\mathbf{V}_{\mathcal{R}} \in \mathbb{C}^{n_{\mathcal{R},t} \times n_{\mathcal{R},b}}$ for the source node and the relay node respectively. These matrices are sometimes unfortunately denoted "precoding" matrices. The number of independent streams of data transmitted from the beamformers is given by $n_{\{\cdot\},b}$ for each node. Consequently, for ideal hardware, the rank of the transmit covariance matrix is given by $n_{\mathcal{S},b}$ and $n_{\mathcal{R},b}$ for the source and relay nodes respectively. The symbols transmitted on each of these transmit beamformers are

given by $\mathbf{s}_{\mathcal{S}} \in \mathbb{C}^{n_{\mathcal{S},b} \times 1}$ and $\mathbf{s}_{\mathcal{R}} \in \mathbb{C}^{n_{\mathcal{R},b} \times 1}$ for the source and relay node respectively. Similarly, the received signal at the destination node under the ideal hardware model is given by

$$\mathbf{z}_{\mathcal{D}} = \mathbf{H}_{\mathcal{R},\mathcal{D}} \mathbf{V}_{\mathcal{R}} \mathbf{s}_{\mathcal{R}} + \mathbf{H}_{\mathcal{S},\mathcal{D}} \mathbf{V}_{\mathcal{S}} \mathbf{s}_{\mathcal{S}} + \mathbf{n}_{\mathcal{D}} , \qquad (2)$$

where $\mathbf{n}_{\mathcal{D}}$ indicates the receiver noise.

As suggested in Section I-C, we will limit the intended rank of the transmit covariance matrices to 1. For low SNR links, this is the optimal water-filling solution [30]. More importantly here, this choice of rank will enable a clearer interpretation of the implication of nonideal effects of the hardware. In addition, we assume that the direct channel between the source and destination $\mathbf{H}_{\mathcal{S},\mathcal{D}}$ is negligible, so that the received signals at the relay and destination become

$$\mathbf{z}_{\mathcal{R}} = \mathbf{H}_{\mathcal{R},\mathcal{R}} \mathbf{v}_{\mathcal{R}} s_{\mathcal{R}} + \mathbf{H}_{\mathcal{S},\mathcal{R}} \mathbf{v}_{\mathcal{S}} s_{\mathcal{S}} + \mathbf{n}_{\mathcal{R}} , \text{ and} \qquad (3)$$

$$\mathbf{z}_{\mathcal{D}} = \mathbf{H}_{\mathcal{R},\mathcal{D}} \mathbf{v}_{\mathcal{R}} s_{\mathcal{R}} + \mathbf{n}_{\mathcal{D}} , \qquad (4)$$

where $\mathbf{v}_{\{\cdot\}}$ indicates the single intended transmit beamformer and $s_{\{\cdot\}}$ indicates the transmitted symbol at a given time.

B. Example Rank-1 Transmission: Twisted SINR Optimization

In general, optimizing the relay system for total capacity is difficult and is made more difficult when hardware imperfections are considered. Here we consider a suboptimal independent optimization approach as an example. While the following approach is suboptimal, it was shown experimentally to have good performance [1]. The approach attempts to maximize a "twisted" signal-to-interference-plus-noise ratio (SINR) by reducing the relay power sent to the relay receiver while directing power to the destination. In particular, the ratio of relay power at the destination node $P_{\mathcal{R},\mathcal{D}}$ to the relay power $P_{\mathcal{R},\mathcal{R}}$ plus noise power at the relay receiver is maximized,

$$\frac{P_{\mathcal{R},\mathcal{D}}}{P_{\mathcal{R},\mathcal{R}} + \sigma_{\mathcal{R},r}^2} = \frac{\langle \| \mathbf{H}_{\mathcal{R},\mathcal{D}} \mathbf{v}_{\mathcal{R}} s_{\mathcal{R}} \|^2 \rangle}{\langle \| \mathbf{H}_{\mathcal{R},\mathcal{R}} \mathbf{v}_{\mathcal{R}} s_{\mathcal{R}} + \mathbf{n}_{\mathcal{R}} \|^2 \rangle}$$

$$= \frac{\rho \, \mathbf{v}_{\mathcal{R}}^\dagger \, \mathbf{H}_{\mathcal{R},\mathcal{D}}^\dagger \mathbf{H}_{\mathcal{R},\mathcal{D}} \, \mathbf{v}_{\mathcal{R}}}{\mathbf{v}_{\mathcal{R}}^\dagger \, (\rho \, \mathbf{H}_{\mathcal{R},\mathcal{R}}^\dagger \mathbf{H}_{\mathcal{R},\mathcal{R}} + \mathbf{I}) \, \mathbf{v}_{\mathcal{R}}} , \qquad (5)$$

where $\| \cdot \|$ is the norm or absolute value, and $\langle \cdot \rangle$ indicates expectation. It is assumed that the relay transmit beamformer is unit normalized $\| \mathbf{v}_{\mathcal{R}} \| = 1$, and the noise-normalized power is indicated by $\rho = \langle \| s_{\mathcal{R}} \|^2 \rangle / (n_{\mathcal{R},r} \, \sigma_{\mathcal{R},r}^2)$, and $\sigma_{\mathcal{R},r}^2$ is the thermal noise power at the relay receiver. The optimized (although suboptimal) relay transmit beamformer is then given by

$$\mathbf{v}_{\mathcal{R}} = \max \text{eigvec} \{ (\rho \, \mathbf{H}_{\mathcal{R},\mathcal{R}}^\dagger \, \mathbf{H}_{\mathcal{R},\mathcal{R}} + \mathbf{I})^{-1} \, \mathbf{H}_{\mathcal{R},\mathcal{D}}^\dagger \mathbf{H}_{\mathcal{R},\mathcal{D}} \} . \qquad (6)$$

C. Example Spatial Receiver: MMSE

The spatial maximum SINR and linear minimum-mean-square-error (MMSE) spatial receivers are the same up to a scaling factor and are therefore equivalent. As an example, the MMSE receive beamformer for the relay node is given by

$$\mathbf{w}_{\mathcal{R}} = \left\langle \mathbf{z}_{\mathcal{R}} \, \mathbf{z}_{\mathcal{R}}^\dagger \right\rangle^{-1} \left\langle \mathbf{z}_{\mathcal{R}} \, s_{\mathcal{S}}^* \right\rangle . \qquad (7)$$

If the transmitter does a good job of protecting the receive array as discussed in Section II-B, then no self-interference component is observed in the receive covariance matrix $\langle \mathbf{z}_\mathcal{R} \mathbf{z}_\mathcal{R}^\dagger \rangle$. However, if signal leaks into the received spatial response of the relay, the receiver will attempt to mitigate the self-interference. Consequently, the number of modes occupied by any eigenvalue spread and the strength of these modes is important.

III. NONIDEAL HARDWARE

The spread of eigenvalues is a useful tool for discussing the effects of nonideal hardware at the relay node. Ideally, in the approach discussed in Section II-B, the receiver would not observe any self-interference. However, significant transmit eigenvalue spread, indicating accidental self-interference, must be spatially mitigated by the receiver. Furthermore, the nonideal artifacts of the receiver front end can further increase the eigenvalue spread that also needs to be mitigated by the receive algorithms.

Under the assumption that the ideal relay transmit covariance matrix $\mathbf{R}_{\mathcal{R},t}$ is rank-1 with a spatial structure given by $\mathbf{v}_\mathcal{R} \mathbf{v}_\mathcal{R}^\dagger$, the nonideal relay transmit covariance[1] by including additional spatial response caused by nonideal transmit effects can be modeled by

$$\mathbf{R}_{\mathcal{R},t} = P_\mathcal{R}\, \mathbf{v}_\mathcal{R} \mathbf{v}_\mathcal{R}^\dagger + \sum_m a_m\, \mathbf{x}_{\mathcal{R},m} \mathbf{x}_{\mathcal{R},m}^\dagger , \qquad (8)$$

where $P_\mathcal{R}$ is the total relay transmit power, and summation is over unintended transmit spatial response with power a_m and spatial response $\mathbf{x}_{\mathcal{R},m} \mathbf{x}_{\mathcal{R},m}^\dagger$.

The self-interference component of the receive covariance $\mathbf{R}_{\mathcal{R},r;SI}$ can be modeled by the sum of the ideal response plus the response caused by transmit and receive errors,

$$\begin{aligned}
\mathbf{R}_{\mathcal{R},r;SI} = &\; P_\mathcal{R}\, \mathbf{H}_{r,r}\, \mathbf{v}_r \mathbf{v}_r^\dagger\, \mathbf{H}_{r,r}^\dagger \\
&+ \sum_m a_m\, \mathbf{H}_{r,r}\, \mathbf{x}_{r,m} \mathbf{x}_{r,m}^\dagger\, \mathbf{H}_{r,r}^\dagger \\
&+ \sum_m b_m\, \mathbf{y}_{r,m} \mathbf{y}_{r,m}^\dagger ,
\end{aligned} \qquad (9)$$

with unintended receive spatial response with power b_m and spatial response $\mathbf{y}_{\mathcal{R},m} \mathbf{y}_{\mathcal{R},m}^\dagger$.

IV. NOISE

The fundamental limit of performance in communication systems is noise. In addition to thermal noise, there is often quantization noise; however, here we will assume that the system is set up such that the thermal noise dominates at the receiver. It is commonly assumed that the thermal noise at the receiver for some node is a complex Gaussian with power $\sigma^2_{\{\cdot\},r} = f_N k_B T B$, where the subscript $\{\cdot\}$ could be $\mathcal{R}$ or $\mathcal{D}$, f_N is the noise figure, k_B is the Boltzmann constant, T is the absolute temperature, and B is the bandwidth (including positive and negative frequencies). The receiver sensitivity can be improved by reducing the noise figure by increasing gain,

---

[1]To be clear, one can construct much more complicated models than considering only the second-order statistics. However, if we constrain the processing to traditional techniques, then this is a reasonable approach.

although this can come at the expense of dynamic range. For some node, the noise component of the receive noise covariance matrix $\mathbf{R}_{\{\cdot\},r;N}$ is given by

$$\mathbf{R}_{\{\cdot\},r;N} = \sigma^2_{\{\cdot\},r}\, \mathbf{I}_{n_{\{\cdot\},r}} . \qquad (10)$$

In some sense, if the self-interference can be mitigated to a level so that receive thermal noise dominates system performance, then one can declare victory.

While it is ignored in most communication systems, there is also a thermal noise component that contributes to the transmitted signal. Because the transmit chain through the hardware is typically operated at a signal level that is large compared to the transmit noise level, the thermal noise contributes little to the transmitted signal, so the receive noise dominates the system's performance. However, for the full-duplex relay node, these small effects are significant to the self-interference mitigation performance. In some work, the effects of nonlinearities are approximated by transmit noise [15], although this is approximation is valid only if higher order nonlinearities are contributing significantly, which is not the model we are considering in this paper. Here, we address nonlinearities explicitly. The significant concern for the relay is that the transmit noise covariance is full rank and thus can overwhelm spatial mitigation at the receiver. For a relay transmit thermal noise level of $\sigma^2_{\mathcal{R},t}$, the thermal noise contribution to the transmit covariance $\mathbf{P}_{\mathcal{R};N}$ for some node is given by

$$\mathbf{P}_{\mathcal{R};N} = \sigma^2_{\mathcal{R},t}\, \mathbf{I}_{n_{\mathcal{R},t}} ; \qquad (11)$$

thus, the transmit noise contribution to the relays receive covariance is the full-rank form $\mathbf{H}_{\mathcal{R},\mathcal{R}} \left(\sigma^2_{\mathcal{R},t} \mathbf{I}_{n_{\mathcal{R},t}} \right) \mathbf{H}_{\mathcal{R},\mathcal{R}}^\dagger$. The fundamental solution to the transmit noise problem is to make sure that it is small compared to the transmit power by reducing the number of potential sources and gain between the digital-to-analog converter and the antennas (implying a higher-power digital-to-analog converter).

V. IQ MISMATCH

Many modern communication systems employ direct conversion architectures for the I and Q channels in which a separate digital-to-analog converter or analog-to-digital converter is employed by the transmitters or receivers respectively. In this case, there is the potential for mismatch between the I and Q channels. Theoretically, a well-designed transmitter can use the knowledge of the transmitted signal to adaptively calibrate. At the receiver, the calibration is more problematic.[2]

Mathematically, the effect of the IQ mismatch can be represented by slight rotations of bases and by slight mismatches in gain that are achieved here by real coefficients $c_1, \cdots, c_4$. These degrees of freedom can be achieved by assuming that some signal $\mathbf{u}$ (that can be used to represent either a transmitted or received signal) is modified by the complex gain term $\mathbf{a}$, and there is a contribution from a complex conjugate

---

[2]In general, the IQ mismatch problem can be addressed by performing all adaptivity in higher dimensional spaces that incorporate the possibility of errors.

term $\mathbf{u}^*$ with amplitude $\mathbf{b}$. Ideally, $\mathbf{a}$ is real, and $\mathbf{b}$ is zero. The signal incorporating IQ mismatch $\mathbf{u}_{\mathrm{IQ}}$ is given by

$$
\begin{aligned}
\mathbf{u}_{\mathrm{IQ}} &= \mathbf{c}_1 \odot \mathbf{u}_{\Re} + \mathbf{c}_2 \odot \mathbf{u}_{\Im} \\
&\quad + i\left[\mathbf{c}_3 \odot \mathbf{u}_{\Re} + \mathbf{c}_4 \odot \mathbf{u}_{\Im}\right] \\
&= (\mathbf{a}_{\Re} + \mathbf{b}_{\Re}) \odot \mathbf{u}_{\Re} + (\mathbf{b}_{\Im} - \mathbf{a}_{\Im}) \odot \mathbf{u}_{\Im} \\
&\quad + i\left[(\mathbf{a}_{\Im} + \mathbf{b}_{\Im}) \odot \mathbf{u}_{\Re} + (\mathbf{a}_{\Re} - \mathbf{b}_{\Re}) \odot \mathbf{u}_{\Im}\right] \\
&= \mathbf{a} \odot \mathbf{u} + \mathbf{b} \odot \mathbf{u}^*, \quad (12)
\end{aligned}
$$

where $\odot$ indicates the Hadamard product, $\cdot_{\Re}$ and $\cdot_{\Im}$ indicate the real and imaginary components of the parameter, under the appropriate substitutions for $\mathbf{c}_1, \cdots, \mathbf{c}_4$.

Under the assumption that the transmitted or observed signal is rank-1, by using the model $\mathbf{u} = \mathbf{v}\, u$, with spatial response $\mathbf{v}$ and random complex signal u, then for typical complex communication signals, we expect that $\langle \mathbf{u}\,\mathbf{u}^\dagger \rangle = P\,\mathbf{v}\,\mathbf{v}^\dagger$ and $\langle \mathbf{u}\,\mathbf{u}^T \rangle = \mathbf{0}$, where P is the total transmit or receive power. The covariance of the transmitted or received signals under these assumptions is given by the rank-2 form,

$$
\begin{aligned}
&\langle (\mathbf{a} \odot \mathbf{u} + \mathbf{b} \odot \mathbf{u}^*)(\mathbf{a} \odot \mathbf{u} + \mathbf{b} \odot \mathbf{u}^*)^\dagger \rangle \\
&= P\,(\mathbf{a} \odot \mathbf{v})(\mathbf{a} \odot \mathbf{v})^\dagger + P\,(\mathbf{b} \odot \mathbf{v})(\mathbf{b} \odot \mathbf{v})^\dagger, \quad (13)
\end{aligned}
$$

although the second eigenvalue is relatively small. IQ mismatch is often discussed in terms of image rejection ratio (IRR). For our vector of random gain $\mathbf{a}$ and distortion $\mathbf{b}$ coefficients, it is given by $\mathrm{IRR} = \langle \|\mathbf{b}\|^2 \rangle / \langle \|\mathbf{a}\|^2 \rangle$.

VI. NONLINEARITY

A. Hard Nonlinearities

The dynamic range in power for linear converters can be approximated by 6 dB for each effective bit. For example, an analog-to-digital converter with 13 effective bits will have a dynamic range of approximately 78 dB, and the number of effects bits available in the hardware keeps growing. If this dynamic range is exceeded, then a harsh, full-rank feature is introduced. While not always possible, here we will assume that we have a sufficient number of effective bits, so that this will not limit our dynamic range. In Section VIII, we show that given model, the assumption bit depth does not limit performance is valid.

B. Soft Nonlinearities

Mixers and amplifiers also introduce "softer" nonlinearities that limit dynamic range. If we assume that the amplifier distortions are nearly symmetric about ground through the use of differential circuits in the signal path, then the errors are dominated by odd terms in the Taylor expansion[3] of the transfer function. Because the lowest distortion terms in the Taylor series tend to dominate, the effects of this distortion is typically characterized by the concept of a third-order intercept (IP3) [31], [32]. If the transfer function is normalized so that the small signal gain is 1, then the intercept point is found by extrapolating the growth of the amplitude of an intermod generated by the interaction between two input tones and the nonlinearity (which grows as the cube of the input signal) and extrapolating to the level at which the linear and the third-order intermod term are equal. For a single-channel example, we assume a nonlinear transfer function $f(\cdot; \{g_m\})$, with some set of Taylor amplitude gain coefficients $\{g_m\}$, For some time-varying signal u, with real, positive amplitude gains g_1 and g_3 for the first- and third-order terms, respectively, the resulting signal u_{NL} is given approximately by

$$
u_{\mathrm{NL}} = f(u; \{g_m\}) \approx g_1\,u - g_3\,u^3. \quad (14)
$$

The input amplitude of the intercept point IIP3 is given by

$$
\mathrm{IIP3} = \sqrt{4g_1/(3g_3)}. \quad (15)
$$

By assuming that the linear gain term is one $g_1 = 1$, and that the third-order nonlinearity is dominated by effects along the separate I and Q paths of a direct conversion architecture, we find the spatial rank of a transmit or receive covariance matrix. Once again, we assume that the intended or observed signal is rank-1, by employing a model $\mathbf{u} = \mathbf{v}\, u$. The direct modulation has separate I and Q channels represented by $\mathbf{u} = \mathbf{u}_{\Re} + i\,\mathbf{u}_{\Im}$. The form for the cube of a vector indicates $\mathbf{v}^3 = \mathbf{v} \odot \mathbf{v} \odot \mathbf{v}$. The third-order distorted signal is given by

$$
\mathbf{u}_{\mathrm{NL}} = \mathbf{v}\, u - g_3\,(\Re\{\mathbf{v}\, u\})^3 - i\,g_3\,(\Im\{\mathbf{v}\, u\})^3. \quad (16)
$$

Because the terms $\mathbf{v}\, u$, $(\Re\{\mathbf{v}\, u\})^3$, and $(\Im\{\mathbf{v}\, u\})^3$ are statistically independent, in general, and have independent spatial responses, the form of the covariance with third-order distortions $\langle \mathbf{u}_{\mathrm{NL}}\,\mathbf{u}_{\mathrm{NL}}^\dagger \rangle$ is rank-3, although the second and third eigenvalues are relatively small. In the case of higher input spatial rank signals, the term $\mathbf{v}\, u$ can be replaced with $\sum_m \mathbf{v}_m\, u_m$, so that in general the initial rank is tripled.

VII. COMBINED RELAY ISOLATION PERFORMANCE

By considering the increase in covariance rank caused by the combination of effects, we will bound the adverse effects from nonideal hardware. As an example, if the receiver employed a zero-forcing approach, every additional self-interference eigenvalue mode would require an additional antenna at the receiver. The worst-case rank due to the original signal is somewhat misleading because it will assume that all effects are strong and spatially distinct; this assumption will wildly overstatement the effects. In Section VIII, we discuss more realistic performance results based on simulation.

For this analysis, we assume the following. The intended transmit spatial signal structure is effectively orthogonal to the relay self-interference channel[4] $\mathbf{H}_{\mathcal{R},\mathcal{R}}$. We assume a direct conversion architecture by both the transmitter and the receiver, and we assume that the transmit noise is small enough and bit depth is large enough that they can be ignored. First, we consider the transmit covariance rank. Here, the intended transmit signal is spatially rank-1. From Equation (13), the transmit IQ imbalance increases the rank by 1, so that it is now 2. Third-order nonlinearities, add two for each degree of freedom, so the transmit rank is 6. At the receiver, the a

---

[3]In general, one would include nonlinear terms and memory.

[4]If there are large additional transmit eigenvalues, a reasonable extension to the discussion in the paper would be to adapt the transmit array to mitigate these as well.

signal of rank-5 is observed (recall that the intended rank-1 signal is orthogonal to the relay self-interference channel). From Equation (12), it is seen that the IQ mismatch doubles the rank, so that the received signal rank is 10. From Equation (16), the third-order nonlinearities for direct conversion triples the rank, extending the rank to 30. As it turns out, this analysis is wildly pessimistic because most of the contributions fall below the received noise floor.

VIII. SIMULATED PERFORMANCE

To simulate the relay system, 9 transmit antennas and 8 receive antennas are assumed. The parameters of the simulation are summarized in Table I. The transmit waveform is a 16 QAM signal with a bandwidth of 40 MHz and with a total average output power of 20 dBm across the 9 transmit antennas. It is assumed that the relay node employs a common local oscillator and therefore phase noise is common mode; thus, the phase noise has no adverse effect on spatial processing. We assume broadband thermal noise in each independent transmit channel on the order of -165 dBc/Hz. Given that each transmit channel on average transmits 10.5 dBm and has a bandwidth of 40 MHz, the transmit SNR is 89 dB. The IRR caused by the IQ mismatch is chosen to be an aggressive -80 dB, which can be achieved through careful calibration. Although each channel had the same IRR, this effect can be achieved with any combination of amplitude and phase errors; therefore, each channel was given a random phase error and the amplitude calculated to achieve the constant IRR of -80 dB.

TABLE I

SIMULATION PARAMETERS

Transmitter	
Noise floor	-154.5 dBm/Hz
SNR (40 MHz bandwidth)	89 dB
Image rejection ratio	-80 dB
Output 3rd-order intercept point	42 dBm
Output 1 dB compression point	32.1 dBm

Receiver	
Noise figure	4 dB
Noise floor (40 MHz bandwidth)	-94 dBm
Image rejection ratio	-40 dB
Input 3rd-order intercept point	-10 dBm

To determine the value of g_3 in Equation (15) for the transmitter, a reasonable output IP3 for the transmitter must be chosen. In many digital modulation systems, gross transmitter distortion is acceptable as long as there is a sufficiently small error vector magnitude (EVM) to properly decode the signal and in most cases this is limited by receiver noise. However, when spatially protecting the relay receiver, much more stringent linearity requirements are necessary. To that end, an output IP3 of 42 dBm is chosen that results in an average EVM of approximately -50 dB. This is quite aggressive but is achievable through the use of a sufficiently linear power amplifier. However, given that the average peak power of each channel is 16.5 dBm and the output compression point is 32.1 dBm, the transmitter is backed off by more than 15 dB from its saturated output power which is relatively inefficient in practice.

By implementing the model of Equation (9) and taking into account the errors of IQ mismatch, third order distortion and noise, an ensemble of eigenvalue distributions of the transmit covariance matrix is simulated. In Figure 1, we display the 10% and 90% curves of the cumulative distribution function (CDF) of the eigenvalues. Because eigenvalues are correlated, this approach is illustrative but not precise. The eigenvalues are plotted in physical power and show that the relay transmitter, as designed, is approximately rank-1 with 20 dBm of total power; however, due to the nonideal transmitters, there is eigenvalue spread. Theory predicts that the rank should grow to 6, but modes 5 and 6 are below the transmit noise floor of -78.5 dBm. By studying the contributions of individual sources of errors, it can be shown that eigenvalues 2 and 3 are dominated by the third-order nonlinearities. The contribution of these nonlinearities is approximately -60 dBc, which is consistent with an EVM of -50 dB given 9 transmit elements (9.5 dB). The fourth eigenvalue is dominated by the IQ mismatch, approximately -80 dBc, which is consistent with an IRR of -80 dBc as discussed in Section V.
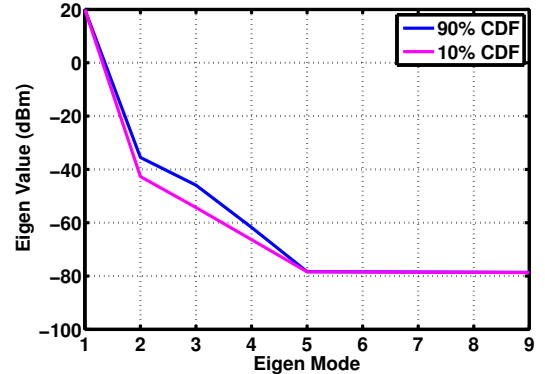
Fig. 1. Eigenvalue distribution of the transmit covariance matrix.

To study the effect of the transmitter deviations from ideal at the spatially protected relay receiver, a self-interference channel with an average of 25 dB attenuation is assumed. The average power incident at any channel in the receive array is approximately -60 dBm, and is therefore reasonably well-protected from self-interference. The receiver is assumed to have IQ mismatch, third-order distortion and noise with the parameters shown in Table I, resulting in a receiver with a 56 dB of spur-free dynamic range.

In Figure 2, we display the 10% and 90% points of the CDF of the eigenvalues of the receive covariance matrix. Despite the nonideal contributions from both the transmitter and receiver, the eigenvalue distribution of the receive covariance matrix is still dominated by the transmitter performance, which is apparent when considering the magnitude of the errors induced by each receiver channel. Because the latent signal present at each receive channel is approximately -60 dBm, the IQ mismatch components incurred by the receiver will be will be at -100 dBm and the third-order distortion will be on the order of -160 dBm, both of which are below the receiver noise floor.

Although theory predicts that the rank will grow to 30 at the receiver, it is clear that the eigenvalues spread above
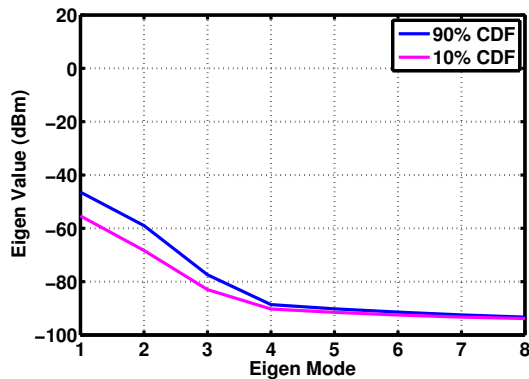
Fig. 2. Eigenvalue distribution of the receive covariance matrix.

the noise floor is relatively modest, well-contained within the first few eigenvalues. Consequently, there is sufficient spatial resources to mitigate the self-interference. These contributions are dominated by the third-order nonlinearites. The contribution of IQ mismatch is surprisingly small. The eigenvalue spread contributions beyond that are produced by transmitter noise shaped by the channel observed just above the receive noise floor.

IX. CONCLUSION

In this paper, we developed a formalism for discussing the spatial suppression of cochannel full-duplex relay self-interference. In particular, we presented a discussion of the phenomenology of the important nonideal hardware effects, and we presented results discussed in the context of the received spatial covariance eigenvalue distribution under realistic system parameters that indicated the viability of the spatial mitigation approach. We would like to thank Dorothy Ryan of MIT Lincoln Laboratory for her helpful comments.

REFERENCES

[1] D. W. Bliss, P. A. Parker, and A. R. Margetts, "Simultaneous transmission and reception for improved wireless network performance," *Conference Proceedings of the IEEE Statistical Signal Processing Workshop*, Aug. 2007.

[2] T. Cover and A. E. Gamal, "Capacity theorems for the relay channel," *IEEE Transactions on Information Theory*, vol. 25, no. 5, pp. 572–584, Sept. 1979.

[3] Y. Y. Kang and J. H. Cho, "Capacity of MIMO wireless channel with full-duplex amplify-and-forward relay," in *IEEE 20th International Symposium on Personal, Indoor and Mobile Radio Communications*, Sept. 2009, pp. 117–121.

[4] V. R. Cadambe and S. A. Jafar, "Degrees of freedom of wireless networks with relays, feedback, cooperation, and full duplex operation," *IEEE Transactions on Information Theory*, vol. 55, no. 5, pp. 2334–2344, May 2009.

[5] Hyungsik Ju, Eunsung Oh, and Daesik Hong, "Catching resource-devouring worms in next-generation wireless relay systems: Two-way relay and full-duplex relay," *IEEE Communications Magazine*, vol. 47, no. 9, pp. 58–65, Sept. 2009.

[6] T. Kwon, S. Lim, S. Choi, and D. Hong, "Optimal duplex mode for DF relay in terms of the outage probability," *IEEE Transactions on Vehicular Technology*, vol. 59, no. 7, pp. 3628–3634, Sept. 2010.

[7] T. Kwon, Y. Kim, and D. Hong, "Comparison of FDR and HDR under adaptive modulation with finite-length queues," *IEEE Transactions on Vehicular Technology*, vol. 61, no. 2, pp. 838–843, Feb. 2012.

[8] C. K. Lo, S. Vishwanath, and R. W. Heath, Jr., "Rate bounds for MIMO relay channels using precoding," in *IEEE Global Telecommunications Conference*, Nov. 2005, vol. 3.

[9] B. Wang, J. Zhang, and A. Host-Madsen, "On the capacity of MIMO relay channels," *IEEE Transactions on Information Theory*, vol. 51, no. 1, pp. 29–43, Jan. 2005.

[10] M. Yuksel and E. Erkip, "Multiple-antenna cooperative wireless systems: A diversity-multiplexing tradeoff perspective," *IEEE Transactions on Information Theory*, vol. 53, no. 10, pp. 3371–3393, Oct. 2007.

[11] S. Katti, S. Gollakota, and D. Katabi, "Embracing wireless interference: Analog network coding," *Proceedings of the ACM SIGCOMM Data Communications Festival*, Aug. 2007.

[12] S. Simoens, O. Munoz-Medina, J. Vidal, and A. del Coso, "On the Gaussian MIMO relay channel with full channel state information," *IEEE Transactions on Signal Processing*, vol. 57, no. 9, pp. 3588–3599, Sept. 2009.

[13] C.-H. Lee, J.-H. Lee, O.-S. Shin, and S.-C. Kim, "Sum rate analysis of multiantenna multiuser relay channel," *IET Communications*, vol. 4, no. 17, pp. 2032–2040, 26 2010.

[14] T. Riihonen, S. Werner, and R. Wichman, "Hybrid full-duplex/half-duplex relaying with transmit power adaptation," *IEEE Transactions on Wireless Communications*, vol. 10, no. 9, pp. 3074 –3085, Sept. 2011.

[15] B. P. Day, A. R. Margetts, D. W. Bliss, and P. Schniter, "Full-duplex MIMO relaying: Achievable rates under limited dynamic range," *IEEE Journal on Selected Areas in Communications*, vol. 30, no. 8, pp. 1541–1553, Sept. 2012.

[16] P. Larsson and M. Prytz, "MIMO on-frequency repeater with self-interference cancellation and mitigation," in *IEEE Vehicular Technology Conference*, April 2009.

[17] T. Riihonen, S. Werner, and R. Wichman, "Spatial loop interference suppression in full-duplex MIMO relays," in *Asilomar Conference on Signals, Systems and Computers*, Nov. 2009, pp. 1508–1512.

[18] Jun Ma, G. Y. Li, Jinyun Zhang, T. Kuze, and H. Iura, "A new coupling channel estimator for cross-talk cancellation at wireless relay stations," in *IEEE Global Telecommunications Conference*, Dec. 2009.

[19] T. Riihonen, S. Werner, and R. Wichman, "Residual self-interference in full-duplex MIMO relays after null-space projection and cancellation," in *IEEE Asilomar Conference on Signals, Systems and Computers*, Nov. 2010, pp. 653–657.

[20] T. Riihonen, S. Werner, and R. Wichman, "Mitigation of loopback self-interference in full-duplex MIMO relays," *IEEE Transactions on Signal Processing*, vol. 59, no. 12, pp. 5983–5993, Dec. 2011.

[21] B. Chun and Y. H. Lee, "A spatial self-interference nullification method for full duplex amplify-and-forward MIMO relays," in *IEEE Wireless Communications and Networking Conference (WCNC)*, April 2010.

[22] J.-H. Lee and O.-S. Shin, "Full-duplex relay based on block diagonalisation in multiple-input multiple-output relay systems," *IET Communications*, vol. 4, no. 15, pp. 1817–1826, 15 2010.

[23] C.-H. Lee, J.-H. Lee, Y.-W. Kwak, Y.-H. Kim, and S.-C. Kim, "The realization of full duplex relay and sum rate analysis in multiuser MIMO relay channel," in *IEEE Vehicular Technology Conference*, Sept. 2010.

[24] D. Choi and D. Park, "Effective self interference cancellation in full duplex relay systems," *Electronics Letters*, vol. 48, no. 2, pp. 129–130, 2012.

[25] D. Senaratne and C. Tellambura, "Beamforming for space division duplexing," in *IEEE International Conference on Communications (ICC)*, June 2011.

[26] B. P. Day, A. R. Margetts, D. W. Bliss, and P. Schniter, "Full-duplex bidirectional MIMO: Achievable rates under limited dynamic range," *IEEE Transactions on Signal Processing*, vol. 60, no. 7, pp. 3702–3713, July 2012.

[27] P. Persson, M. Coldrey, A. Wolfgang, and P. Bohlin, "Design and evaluation of a 2 x 2 MIMO repeater," in *European Conference on Antennas and Propagation (EuCAP)*, Mar. 2009, pp. 1509–1512.

[28] K. Haneda, E. Kahra, S. Wyne, C. Icheln, and P. Vainikainen, "Measurement of loop-back interference channels for outdoor-to-indoor full-duplex radio relays," in *European Conference on Antennas and Propagation (EuCAP)*, April 2010.

[29] T. Riihonen, A. Balakrishnan, K. Haneda, S. Wyne, S. Werner, and R. Wichman, "Optimal eigenbeamforming for suppressing self-interference in full-duplex MIMO relays," in *Conference on Information Sciences and Systems (CISS)*, March 2011.

[30] D. W. Bliss, K. W. Forsythe, A. O. Hero, and A. F. Yegulalp, "Environmental issues for MIMO capacity," *IEEE Transactions on Signal Processing*, vol. 50, no. 9, pp. 2128–2142, Sept. 2002.

[31] Behzad Razavi, *RF Microelectronics*, Pearson Education, Upper Saddle River, New Jersey, 2011.

[32] David M. Pozar, *Microwave Engineering*, John Wiley & Sons, Hoboken, New Jersey, 2005.